Supporting Information

Cooke et al. 10.1073/pnas.0900517106

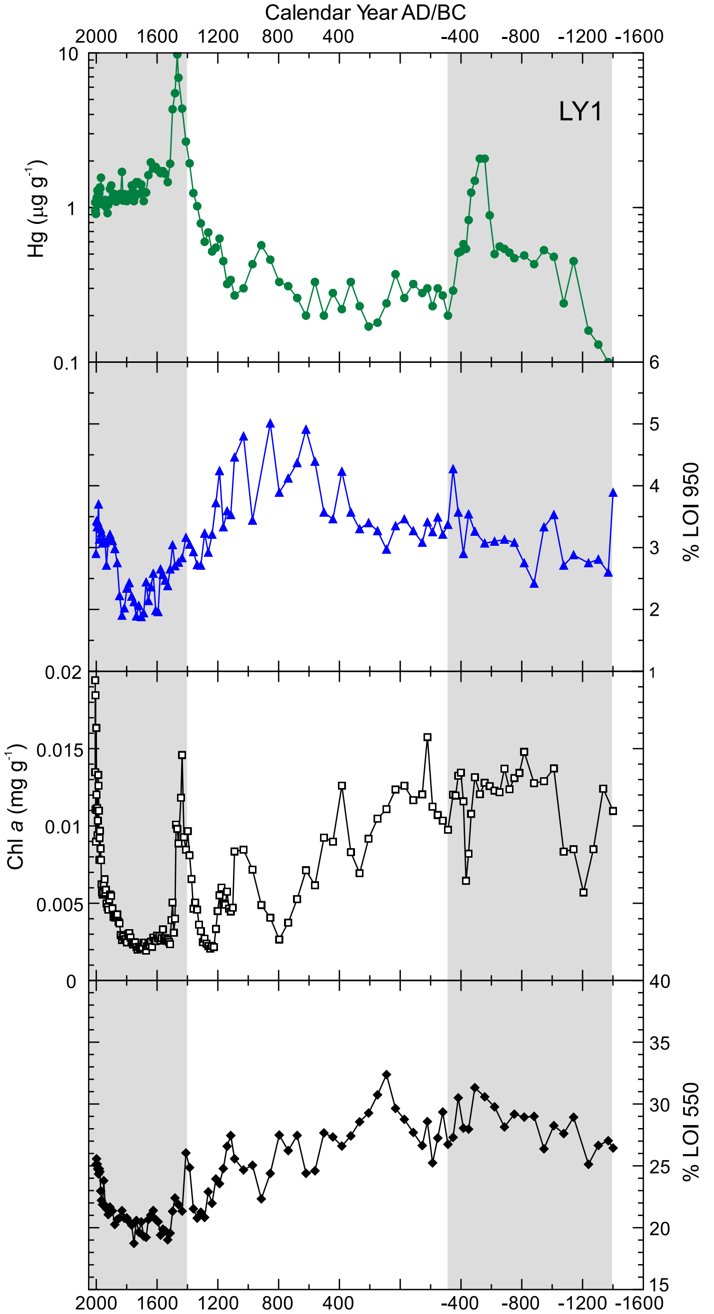

Fig. S1. Geochemical and organic matter profiles from core LY1. Significant increases in Hg are shaded and cannot be attributable to rapid increases in other sediment variables. Both within-lake primary production and total organic mater burial have been shown to influence the accumulation of Hg within lake sediments [Outridge PM, et al. (2007) *Environ Sci Tech* 41:5259–5265]. There is no correlation between Hg and Chl *a* ($r^2 = 0.01$), and Hg and % LOI 550 ($r^2 = -0.15$). The exception is an obvious large peak in both Hg and Chl *a* centered at *ca.* 1450 AD. However, similar Chl *a* concentrations (e.g., *ca.* 200 BC) yield no net increase in Hg, and no increase in Hg is noted in modern sediments when Chl *a* attains its highest levels (0.02 mg/g).

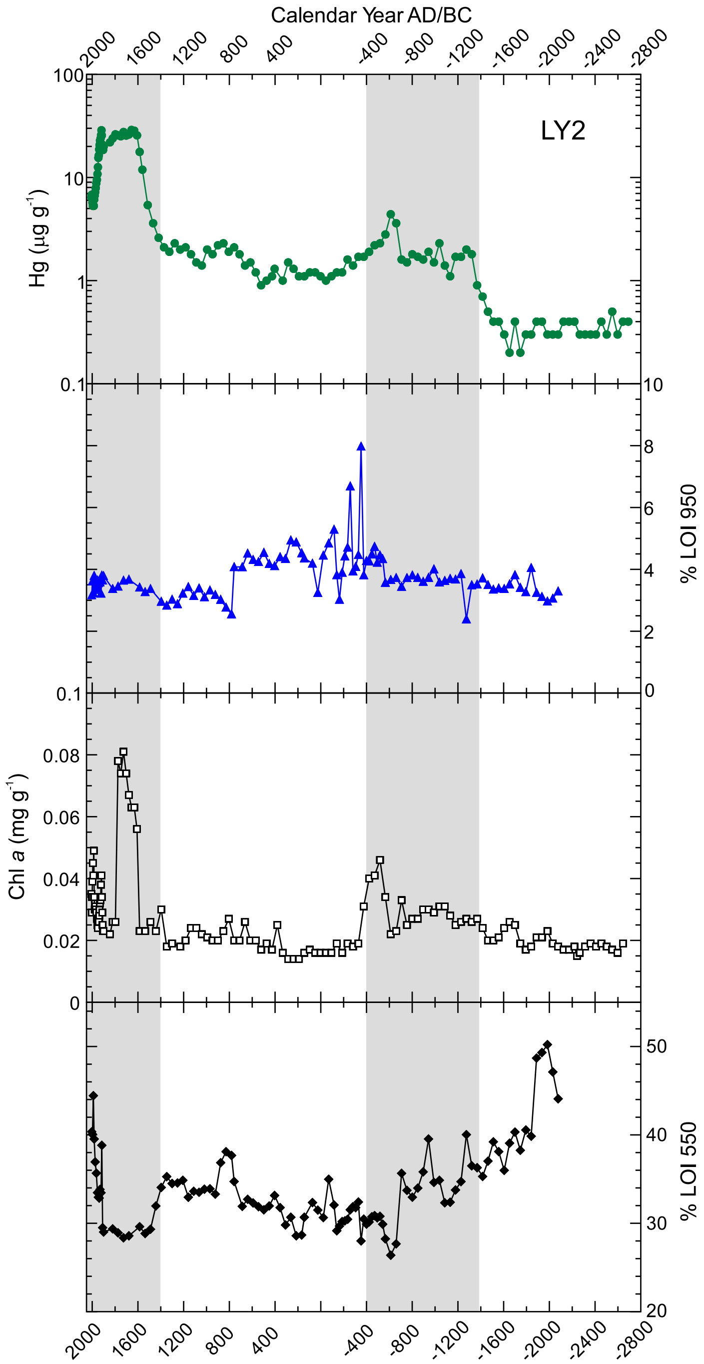

Fig. S2. Geochemical and organic matter profiles from core LY2. As observed at LY1, increases in Hg are shaded and cannot be attributable to rapid increases in other sediment variables.

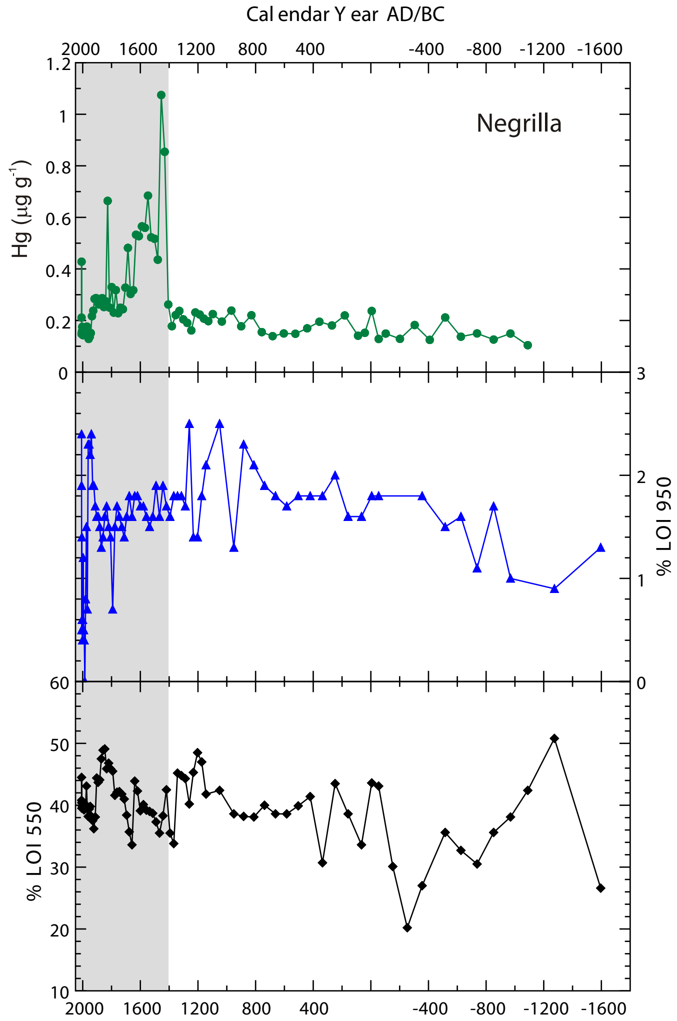

Fig. S3. Geochemical and organic matter profiles from Negrilla. As with LY1 and LY2, increases in Hg are shaded and cannot be attributable to rapid increases in other sediment variables.

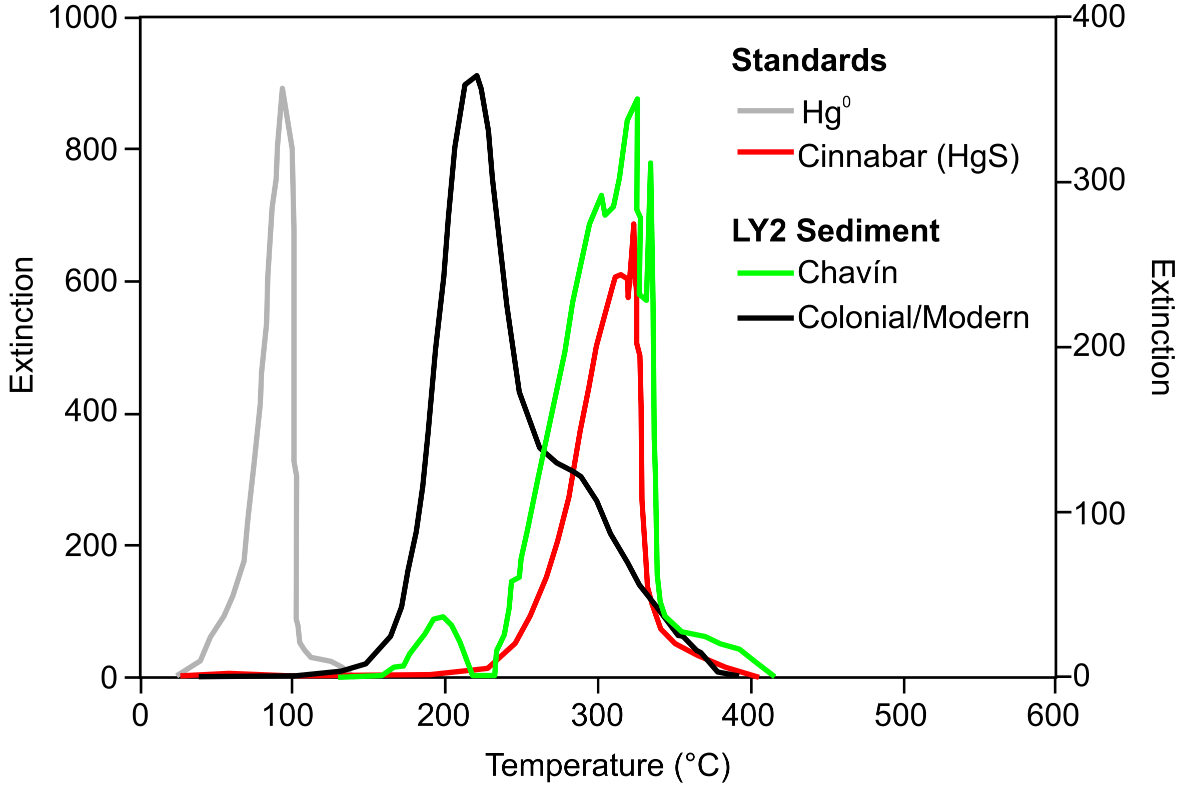

Fig. S4. Solid-phase Hg thermo-desorption curves of standard materials and selected sediment samples of the LY2 core. The Chavín and Colonial/Modern samples are from 80 and 8.5 cm depth respectively. The Colonial/Modern sample-peak lies between Hg^0 and cinnabar, indicating the presence of matrix-bound Hg, a fraction which is largely bound to organic matter, but may also include particulate-bound Hg (1). Cinnabar and Hg^0 standard samples were obtained from the Idrija mercury mine, Slovenia (2).

1. Biester H, Scholz C (1997) Determination of mercury binding forms in contaminated soils: mercury pyrolysis versus sequential extractions. *Environ Sci Tech* 31:233–239.
2. Biester H, Gosar M, Covelli S (2000) Mercury speciation in sediments affected by dumped mining residues in the drainage area of the Idrija mercury mine, Slovenia. *Environ Sci Tech* 34:3330–3336.

Table S1. Down-core ^{210}Pb activities, calculated CRS sediment ages, and CRS sediment accumulation rates for the three study cores

Depth Interval, cm	^{210}Pb activity, Bq·g^{-1}	Error ^{210}Pb activity (1 σ)	CRS age	Error age (1 σ)	CRS sed. accum. rate, g·m^{-2}·year^{-1}	Error SAR (1 σ)
			Laguna Yanacocha 1 (LY1)			
0–0.5	0.673	0.021	2007	0	367	19
1–1.5	0.529	0.016	2005	0	442	22
2–2.5	0.301	0.017	2002	1	737	70
3–3.5	0.258	0.013	1998	1	783	69
4–4.5	0.273	0.014	1994	1	653	59
5–5.5	0.255	0.010	1990	1	613	44
6–6.5	0.255	0.010	1985	2	529	37
7–7.5	0.193	0.008	1980	2	638	53
8–8.5	0.181	0.004	1976	2	599	32
9–9.5	0.143	0.007	1971	4	703	75
10–10.5	0.137	0.007	1966	5	642	71
11–11.5	0.125	0.007	1959	6	579	71
12–12.5	0.141	0.007	1951	6	378	40
13–13.5	0.086	0.006	1941	12	585	108
14–14.5	0.076	0.005	1933	15	573	116
16–16.5	0.072	0.004	1910	22	312	69
18–18.5	0.052	0.003				
20–20.5	0.038	0.003				
30–30.5	0.032	0.003				
40–40.5	0.037	0.003				
			Laguna Yanacocha 2 (LY2)			
0.5–1	1.060	0.032	2004	0	91	4
1.5–2	0.754	0.030	1998	1	107	6
2.5–3	0.628	0.016	1990	1	102	4
3.5–4	0.562	0.015	1983	1	91	4
4.5–5	0.434	0.012	1974	2	89	4
5.5–6	0.315	0.006	1964	2	93	3
6.5–7	0.191	0.004	1954	2	120	5
7.5–8	0.128	0.003	1946	4	149	9
8.5–9	0.096	0.005	1939	8	174	19
9.5–10	0.099	0.005	1932	8	133	14
10.5–11	0.070	0.004	1923	12	165	24
11.5–12	0.055	0.003	1916	18	193	39
12.5–13	0.049	0.003	1909	25	190	48
13.5–14	0.052	0.004	1901	24	134	30
14.5–15	0.047	0.003	1890	29	115	28
16.5–17	0.034	0.003				
18.5–19	0.031	0.002				
20.5–21	0.027	0.002				
30–30.5	0.024	0.002				
40–40.5	0.021	0.002				
			Laguna Negrilla			
0–0.5	1.361	0.099	2008	0	145	16
1–1.5	0.793	0.060	2006	0	239	29
2–2.5	0.800	0.032	2004	0	223	16
3–3.5	0.711	0.032	2002	1	234	18
4–4.5	0.881	0.034	1999	1	171	11
5–5.5	0.851	0.036	1995	1	158	12
6–6.5	0.840	0.035	1992	1	143	10
7–7.5	0.877	0.037	1988	1	120	9
8–8.5	0.678	0.021	1983	2	137	9
9–9.5	0.400	0.015	1979	3	218	20
10–10.5	0.468	0.017	1976	3	168	14
12–12.5	0.403	0.017	1969	4	157	15
14–14.5	0.400	0.018	1959	5	118	12
16–16.5	0.335	0.019	1948	8	102	13
18–18.5	0.251	0.011	1935	10	94	13
20–20.5	0.189	0.012	1913	19	69	14
22–22.5	0.073	0.006	1886	114	162	151
25–25.5	0.075	0.004	1879	107	120	100
30–30.5	0.058	0.004				
45–45.5	0.035	0.003				

Table S2. Table of radiocarbon determinations for the three study cores

UCI ID	Lake	Depth, cm	Sample size, mg of C	^{14}C age BP	2 σ calibrated range	Median date
51338	LY1	45.5–46.5	0.10	520 ± 15	1420–1450 AD	1435 AD
49762	LY1	60–60.5	0.21	1020 ± 20	1020–1150 AD	1090 AD
44752	LY1	80–82	0.11	2175 ± 25	345–50 BC	145 BC
49764	LY1	90.5–91	0.18	2460 ± 20	730–400 BC	475 BC
49763	LY1	95.5–96	0.11	2675 ± 25	835–675 BC	800 BC
51339	LY2	36–37.5	0.04	1285 ± 30	690–885 AD	790 AD
49759	LY2	56–57.5	0.18	2225 ± 20	360–115 BC	260 BC
49760	LY2	87.5–89.5	0.14	3390 ± 20	1690–1525 BC	1620 BC
51337	Negrilla	49.5–50	0.16	3170 ± 15	1450–1610 AD	1465 AD
56388	Negrilla	87.5–88	0.04	2060 ± 45	165 BC–115 AD	10 BC
49765	Negrilla	112.5–114	0.05	440 ± 45	1495–1260 BC	1390 BC

Table S3. Table of blank values, average relative standard deviations, and recoveries of standard reference materials associated with DMA80 measurement of Hg

	LY1	LY2	Negrilla
Blanks, ng/g (*n*)	1.4 (25)	4.0 (14)	0.5 (24)
Duplicates, avg. % difference (*n*)	15% (14)	12% (10)	4% (20)
MESS-3, avg. % recovery (*n*)	101% (11)	100% (7)	97% (14)
PACS-2, avg. % recovery (*n*)	97% (11)	101% (6)	101% (11)